Negative Ion Electrospray of Bromo- and Chloroacetic Acids and an Evaluation of Exact Mass Measurements with a Bench-Top Time-of-Flight Mass Spectrometer

Olivier Debré*
National Research Council Postdoctoral Research Associate, Cincinnati, Ohio, USA

William L. Budde
U. S. Environmental Protection Agency, Office of Research and Development, Cincinnati, Ohio, USA

Xinbei Song†
Oak Ridge Institute for Science and Education Postdoctoral Research Associate, Cincinnati, Ohio, USA

The negative ion electrospray mass spectra of six bromo- and chloroacetic acids were measured using two different electrospray interfaces and single quadrupole and bench-top time-of-flight mass spectrometers. With each acid at 50 μg/mL in aqueous methanol at pH 10, the anions observed included deprotonated molecules, adducts, and fragment ions. With each acid at 100 ng/mL in aqueous acetonitrile at pH 10, mainly deprotonated molecules are observed. The exact *m/z* measuring capability of the time-of-flight mass spectrometer was evaluated to assess the potential for the determination of the individual acids in mixtures without an on-line separation. Mean measurement errors were nearly always less than $\pm$ 9 ppm and the majority were less than $\pm$ 5 ppm. Potential interferences by substances having similar exact masses and the ability to form anions in aqueous solutions were evaluated. The estimated detection limits of the five regulated haloacetic acids in drinking water, without a sample preconcentration step, are in the range of 24–86 ng/mL, which is within about a factor of 10 of the levels required for routine monitoring of the acids. Actual drinking water samples were not analyzed pending the development of slightly more sensitive techniques and quantitative analytical procedures. (J Am Soc Mass Spectrom 2000, 11, 809–821) © 2000 American Society for Mass Spectrometry

The disinfectants chlorine, chloramine, chlorine dioxide, and ozone are used to control bacteria, protozoa, and viruses in treated drinking water. Disinfection byproducts (DBPs) are formed when these disinfectants react with aquatic humic substances and other natural organic material and produce chlorinated or oxygenated organic compounds [1]. Although ozone disinfection is growing in popularity, disinfection with chlorine is by far the most common scenario in the United States and some other countries. When bromide ion is present in the source water, as it is in most surface and ground waters, chlorine oxidizes bromide to generate very reactive bromine atoms which produce brominated and mixed bromochloro DBPs. When the bromide ion concentration is relatively high, as it is in some coastal areas and ground waters, brominated compounds dominate the distribution of DBPs [1].

The bromo-, chloro-, and bromochloroacetic acids, which are commonly called haloacetic acids, are one class of DBPs found in drinking water [1]. The nine possible haloacetic acids containing only Br and/or Cl are shown in Scheme 1 along with the abbreviations used in this article. The U. S. Environmental Protection Agency (USEPA) has classified dichloroacetic acid (DCAA) as a probable human carcinogen and trichloroacetic acid (TCAA) as a possible human carcinogen [2]. A maximum contaminant level (MCL) of 60 μg/L for the sum of the concentrations of monochloroacetic acid (MCAA), DCAA, TCAA, monobromoacetic acid (MBAA), and dibromoacetic acid (DBAA) is promulgated in federal regulations for drinking water in the United States [3]. Actual concentrations found in drinking water supplies vary widely but median values of the sum of the concentrations of these five acids were

Address reprint requests to Dr. William L. Budde, USEPA, 26 W. Martin L. King Drive, Cincinnati, OH 45268. E-mail: Budde.William@epa.gov

* Present address: Institut de Physique Nucleaire, University Claude Bernard, Villeurbanne, France 69622.

† Present address: Procter and Gamble Co., Ivorydale Technical Center, Cincinnati, OH 45217.

1044-0305/00/$20.00
PII S1044-0305(00)00147-1

Received December 13, 1999
Revised May 11, 2000
Accepted May 11, 2000

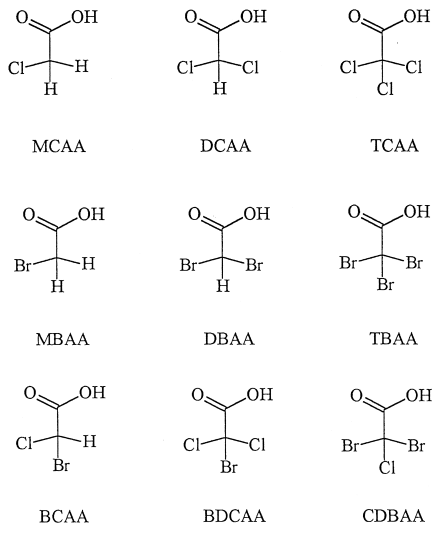

Scheme 1

reported to be 13–21 μg/L in one study [1]. Substances with MCLs in drinking water are commonly said to be *regulated*. The three mixed bromochloroacetic acids were not included in this study and they are not regulated.

Essentially all of the published data on the concentrations of this series of acids in drinking water has been obtained by either liquid–liquid or liquid–solid–liquid partitioning of the acids into an organic solvent at a pH of 2 or lower, conversion of the acids into volatile methyl esters, and gas chromatography (GC) with an electron capture detector (ECD) [4–6]. Approximately 8 h are required to prepare a group of 8–12 samples for GC/ECD and the extractions, extract concentrations, and derivatization reactions must be conducted with considerable care and skill to avoid losses of the analytes. The potential for false positives with this method is relatively high because of the widespread use of the selective but nonspecific ECD detector.

The purpose of this research was to determine the negative ion electrospray (ES) mass spectra of six haloacetic acids at low parts-per-million to low parts-per-billion concentrations in several aqueous organic solvent solutions. Spectra were acquired with different types of electrospray interfaces on a single quadrupole and a bench-top reflection time-of-flight mass spectrometer. The collision induced dissociations (CIDs) of the acid anions were studied with both instruments and the accuracy and precision of exact *m/z* measurements were determined with the time-of-flight spectrometer. Another purpose of this research was a preliminary exploration of the potential for the rapid determination of the regulated acids as their anions in water using ES/mass spectrometry (ES/MS). This approach could potentially obviate the relatively slow and nonspecific method currently used for measurement of the haloacetic acid DBPs in drinking water.

Experimental

Materials

The six haloacetic acids, flavianic acid hydrate, and 2-naphthoxyacetic acid were purchased from Aldrich (Milwaukee, WI) with stated purities of 97–99%. Trichloroacetic acid was also purchased from Fisher Scientific (Fair Lawn, NJ) with a stated purity of 100% and dibromoacetic acid was also purchased from Fluka (Ronkonkoma, NY) with a purity stated at $>$ 97%. Trifluoroacetic acid was peptide synthesis grade and was purchased from Applied Biosystems (Foster City, CA). Fluorescein was purchased from Avocado Research Chemical Ltd. (Heysham, Lancashire, UK) with a stated purity of 99%. All materials were used without purification. Optima grade acetonitrile and methanol and certified American Chemical Society plus grade ammonium hydroxide were purchased from Fisher Scientific and de-ionized water was obtained from Milli-Q water system (Millipore, Bedford, MA). Uncoated fused silica capillaries (FSCs) were purchased from Polymicro Technologies (Phoenix, AZ).

Instrumentation

The single quadrupole mass spectrometer was a Hewlett-Packard (Palo Alto, CA) model 5989B equipped with a Hewlett-Packard model 59987A ES ion source. Some components of the ES ion source (model 103313 serial number 1066) were manufactured by Analytica of Branford (Branford, CT) including a CE-Pro capillary electrophoresis (CE) probe. This ES ion source has a design similar to that described by Fenn et al., in which the electrospray needle is at ground potential and high voltage (HV) is applied to the cylindrical and endplate electrodes and to the entrance of a dielectric glass capillary leading to the mass spectrometer [7]. The ends of the dielectric capillary are coated with a thin layer of Pt to facilitate connection of the electrical leads. The tip of the spray needle is located a few millimeters from the entrance to the dielectric capillary and is positioned for optimum ion detection and spray stability. The CE/ES probe contains three concentric tubes whose functions are described in the next paragraph. The CE/ES probe and the ES interface have been described in detail [8]. The original optics of the ion source were replaced with an Iris hexapole ion guide (Analytica of Branford) to improve transmission of low *m/z* species. The mass spectrometer was equipped with a high energy conversion dynode detector and a G1034C MS ChemStation data system.

Analyte solutions were introduced into the Hewlett-Packard ES ion source using the pressure mode of a Crystal 300 CE instrument (Thermo Capillary Electrophoresis; Franklin, MA) as a substitute for a second syringe pump which was not available. No HV was applied to the CE anode and the analyte solutions were infused into the CE/ES probe through a 75-μm i.d. $\times$

75-cm uncoated FSC. A Harvard Apparatus (South Natick, MA) Model 55-2222 syringe pump was used to deliver 4–6 μL/min of methanol to the CE probe where it is used as a sheath liquid around the outside of the FSC. The sheath liquid provides sufficient liquid flow to maintain a stable ES and provides a connection to ground between the analyte solution and the stainless-steel tube. A stream of oxygen gas at 100 mL/min flows between the intermediate and the outer concentric stainless-steel tubes of the CE/ES probe. This gas assists in the nebulization of the liquid flow and prevents corona discharge by capturing stray electrons. The electrospray HV was 3300 V on the larger outer cylindrical electrode, 3000 V on the smaller endplate electrode, and 3300 V on the capillary entrance. A flow of heated dry nitrogen gas (heater temperature 180 °C) was maintained counter to the ES flow to promote solvent vaporization and desolvation of the negative ions. The spectrometer was repetitively scanned from 50 to 350 *m/z* at about 0.4 s/scan.

The bench-top reflection time-of-flight (TOF) mass spectrometer was a PE Biosystems (Framingham, MA) Mariner model equipped with a PE Biosystems ES ion source. The ES source design is similar to that described by Bruins et al. in which a potential of ± 2–3 kV is applied to a stainless-steel spray needle [9]. The tip of the spray needle is located a few millimeters from an orifice leading to the mass spectrometer and is positioned for optimum ion detection and spray stability. The ES needle was assembled in this laboratory from commercially available parts and consists of three concentric tubes. The innermost tube is a 40-μm i.d. × 105-μm o.d. FSC, which contains the sample flow. The FSC is surrounded by a 0.005-in. i.d. × 0.020-in. o.d. stainless-steel tube from Upchurch Scientific (Oak Harbor, WA) and this intermediate tube is surrounded by a 0.030-in. i.d. × 0.0625-in. o.d. stainless-steel tube from Upchurch. The FSC extended through the intermediate stainless-steel tube and projected about 1 mm beyond the tip of the needle. The functions of these tubes are the same as described for the Hewlett-Packard ion source. Ions are injected orthogonal to the flight tube and push and pull electrodes accelerate the ions in rapid pulses into the flight tube. The field-free flight tube is 0.6 m followed by a second-order electrostatic mirror and a return path to a microchannel ion detector giving an effective path length of 1.3 m for the TOF analyzer. Resolving powers of 3500–4000 based on the full-peak width at half-peak height definition were routinely used and resolving powers up to about 5000 were occasionally obtained and used.

With the TOF system analyte solutions are introduced into the FSC at 0.5–1 μL/min with the Harvard Apparatus syringe pump. The instrument's internal syringe pump was used to deliver 2–3 μL/min of methanol or acetonitrile as a sheath liquid between the FSC and the inner stainless-steel tube. The sheath liquid provides sufficient liquid flow to maintain a stable ES and provides an electrical connection between the high voltage on the metal tube and the analyte solution. A stream of ultrahigh purity oxygen gas at 300–900 mL/min flowed between the intermediate and outer stainless-steel concentric tubes. This gas assists in the nebulization of the liquid flow and prevents corona discharge by capturing stray electrons. The electrospray HV of − 2600 V was applied to the stainless needle and a flow of dry nitrogen gas was maintained counter to the ES flow to promote solvent vaporization and desolvation of the negative ions. The analyzer *m/z* range was set at 10–9000 and spectra were accumulated over a period of 10 s. Ten 10-s accumulations were then mass calibrated and the results from the ten spectra averaged to give the data reported in this article.

Analyte Solutions

Analyte solutions were prepared in volumetric flasks by dissolving an accurately weighed amount of the acid or internal standard in de-ionized water. Multianalyte solutions were prepared by mixing aliquots of individual solutions and diluting with de-ionized water. Before analysis a 50- or 100-mL portion of a multianalyte solution was adjusted to pH 10 by addition of 25–50 μL of ammonium hydroxide. A 1 mL aliquot of the mixed analyte solution at pH 10 was then mixed with 1 mL of either methanol or acetonitrile.

Results and Discussion

The flow injection negative ion ES mass spectra of five haloacetic acids were measured with the quadrupole mass spectrometer system and each acid at 50 μg/mL (50 ppm) in 50% (v/v) methanol–water at pH 10. An operational variable of this ES interface is the voltage applied to the exit of the dielectric capillary (Cap ex) which transports ions from the spray chamber to the mass spectrometer. The pressure in the region between the capillary exit and a skimmer is about 1 torr and ions that emerge from the capillary may undergo collisions that cause desolvation, declustering, and some fragmentation of the anions. The negative ion ES spectra of the five acetic acids were measured at Cap ex voltages of − 40, − 60, − 80 and − 100 V. The ions and their relative abundances in the spectra of the five acids are shown in Table 1 as a function of Cap ex voltage. Where groups of ions caused by naturally occurring isotopes are observed, only the most abundant ion of the group is shown in the table.

The flow injection negative ion ES mass spectra of the same five haloacetic acids, and tribromoacetic acid (TBAA), were measured at the same concentration, 50 ppm of each acid, in the same solvent, and at the same pH with the TOF mass spectrometer system. This instrument system was capable of detecting the analytes at lower concentrations than the quadrupole instrument system and, in order to utilize the same concentrations and obtain comparable data, an adjustment was made to avoid saturation of the instrument

Table 1. Relative abundances of negative ions in the ES mass spectra of haloacetic acids measured with the quadrupole instrument system as a function of Cap ex voltages

Analyte	$V_{Cap\ ex}$ (V)	$(M–H)^-$ (%)	$(2M–H)^-$ (%)	$(M–CO_2–H)^-$ (%)
MCAA	− 40	61	100	0
	− 60	100	46	0
	− 80	100	10	0
	− 100	[a]	[a]	[a]
DCAA	− 40	100	48	0
	− 60	100	27	8
	− 80	100	0	0
	− 100	50	0	100
TCAA	− 40	45	94	100
	− 60	45	84	100
	− 80	76	39	100
	− 100	28	0	100
MBAA	− 40	100	35	0
	− 60	100	18	0
	− 80	100	0	0
	− 100	[a]	[a]	[a]
DBAA	− 40	100	26	0
	− 60	100	22	20
	− 80	89	4	100
	− 100	33	0	100

[a]Not measured.

electronics. The distance between the tip of the spray needle and the ion entrance orifice was increased by a few millimeters to reduce the signal intensities and prevent saturation. Three operational variables in the TOF instrument system ES interface are: the voltages applied to the nozzle (N), the first skimmer (S), and the quadrupole assembly (Q). The pressure in the region between the nozzle and the first skimmer is not available but is reported by the manufacturer of the instrument to be below atmospheric pressure. Ions that emerge from the nozzle are accelerated toward the skimmer by the potential difference $V_S - V_N$ and may undergo CID in this region. A second region where CID may occur is between the first skimmer and the quadrupole assembly. The measured pressure in this region is 1.5×10^{-2} torr and the potential difference is designated $V_Q - V_S$.

The negative ion ES spectra of the six acetic acids were measured at a series of $V_S - V_N$ and $V_Q - V_S$ values and the ions observed and their relative and absolute abundances (ion counts/second (cts/s)) are shown in Table 2. Again, where groups of ions caused by naturally occurring isotopes are observed, only the most abundant ion of the group is shown in the table. The column on the far right of Table 2 also shows for each compound and voltage setting the quantity N_{mono}, which is twice the absolute abundance of the proton bound dimer ion plus the sum of the absolute abundances of all other ions. This is a measure in terms of monomer ions of the total ion abundance in each spectrum. Figure 1 shows the changes in absolute abundances of the ions from the six acids as a function of $V_S - V_N$. Plots of ion abundances as a function of $V_Q - V_S$, which are not shown, are very similar.

The haloacetic acids gave three types of negative ions with the two instrument systems: $(M–H)^-$ ions, $(2M–H)^-$ proton bound dimer ions, and $(M–CO_2–H)^-$ ions. The pK_a in water of each acid is shown near the abbreviation of the acid in Figure 1 [10]. Since all pK_a are $\ll$ than the solution pH, complete dissociation of the acids in 50% methanol–water solution is expected. However, ammonia and methanol are most likely evaporated rapidly in the aerosol spray and the pH within the aerosol droplets is probably lower than in the bulk sample solution, but still high enough to ensure a significant degree of ionization of the acids. Therefore the relative abundances of the $(M–H)^-$ ions could be expected to show some relationship to the pK_a values of the acids.

All the acids measured with the quadrupole system gave relatively abundant $(M–H)^-$ ions in the range of 28–100% depending on the Cap ex voltage (Table 1). With the TOF instrument system, $(M–H)^-$ ions are most abundant in the spectra of DCAA, MBAA, and DBAA at relatively low values of $V_S - V_N$ and $V_Q - V_S$ (Figure 1 and Table 2), but this ion is not observed with MCAA and TBAA. The acid DCAA is stronger than MCAA and the DCAA spectrum is dominated by very abundant $(M–H)^-$ ions at the lower $V_S - V_N$ and $V_Q - V_S$ values (Figure 1 and Table 2).

The only ion observed with MCAA in the TOF system is the low absolute abundance proton bound dimer $(2M–H)^-$ formed by association of an $(M–H)^-$ ion with a MCAA molecule (first reaction in Scheme 2). This proton bound dimer is also the base peak in the spectrum of MCAA measured on the quadrupole system but only at the lowest Cap ex voltage (Table 1). Chloroacetic acid is the weakest of the chlorinated acetic acids with a pK_a of 2.85 in water [10] and the single chlorine atom may not have sufficient electron withdrawing power to cause complete dissociation of the proton bound dimer in the ammonia depleted droplets. Increasing the Cap ex voltage with the quadrupole system decreases the $(2M–H)^-$ ion relative abundance and the $(M–H)^-$ ion becomes the base peak (Table 1). By contrast, when $V_S - V_N$ and $V_Q - V_S$ are increased in the TOF system, the proton bound dimer decreases in absolute abundance without the appearance of other ions (Figure 1 and Table 2). Ions from MCAA were no longer observable when $V_S - V_N$ was > 45 V. At the higher $V_S - V_N$ and $V_Q - V_S$ values, the MCAA $(2M–H)^-$ ions are dissociated but the $(M–H)^-$ ions are neutralized by combining with a proton from the solvent system. The behavior of MCAA in 50% methanol–water is anomalous as MBAA, which has a similar pK_a of 2.9 in water [10], behaves as expected, and gives mainly $(M–H)^-$ ions with both systems (Figure 1 and Tables 1 and 2).

Proton bound dimers are generally observed at moderate to higher relative abundances in spectra measured with the quadrupole system at the lower Cap ex volt-

Table 2. Relative and (absolute) abundances of negative ions in the ES mass spectra of haloacetic acids measured with the TOF instrument system at various nozzle (V_N), skimmer (V_S), and quadrupole (V_Q) voltages

Analyte	$V_S - V_N$ (V)	$V_Q - V_S$ (V)	$(M–H)^-$	$(2M–H)^-$	$(M–CO_2–H)^-$	N_{mono}
MCAA	31	1.0	0	100 (38)	0	76
	46	1.0	0	100 (15)	0	30
	31	1.0	0	100 (38)	0	76
	31	3.5	0	100 (15)	0	30
DCAA	31	1.0	100 (217)	4 (9)	0	235
	46	1.0	100 (219)	2 (5)	0	229
	61	1.0	100 (249)	2 (4)	0	257
	76	1.0	100 (56)	3 (2)	0	60
	91	1.0	100 (5)	13 (1)	0	7
	31	1.0	100 (312)	5 (15)	0	342
	31	3.5	100 (280)	3 (9)	0	298
	31	6.0	100 (169)	1 (2)	0	173
	31	8.5	100 (98)	1 (1)	0	100
	31	11.0	100 (51)	2 (1)	0	53
TCAA	31	1.0	23 (52)	6 (13)	100 (223)	301
	46	1.0	12 (26)	4 (9)	100 (226)	270
	61	1.0	4 (5)	1 (1)	100 (126)	133
	76	1.0	0	0	100 (52)	52
	91	1.0	0	0	100 (11)	11
	31	1.0	23 (58)	6 (15)	100 (250)	338
	31	3.5	16 (38)	4 (10)	100 (235)	293
	31	6.0	17 (25)	3 (4)	100 (152)	185
	31	8.5	18 (20)	1 (1)	100 (110)	132
	31	11.0	26 (11)	0	100 (42)	53
MBAA	31	1.0	100 (294)	9 (26)	0	346
	46	1.0	100 (327)	4 (13)	0	353
	61	1.0	100 (150)	0	0	150
	76	1.0	100 (25)	0	0	25
	31	1.0	100 (281)	9 (25)	0	331
	31	3.5	100 (241)	6 (14)	0	269
	31	6.0	100 (170)	3 (4)	0	178
	31	8.5	100 (109)	1 (1)	0	110
	31	11.0	100 (69)	0	0	69
DBAA	31	1.0	100 (422)	3 (12)	1 (3)	449
	46	1.0	100 (407)	2 (8)	20 (81)	504
	61	1.0	70 (225)	0	100 (321)	546
	76	1.0	12 (53)	0	100 (431)	484
	91	1.0	2 (4)	0	100 (283)	287
	106	1.0	0	0	100 (117)	117
DBAA	31	1.0	100 (416)	2 (10)	1 (3)	439
	31	3.5	100 (428)	2 (9)	15 (65)	511
	31	6.0	100 (334)	1 (3)	47 (158)	498
	31	8.5	86 (228)	0	100 (264)	492
	31	11.0	40 (148)	0	100 (369)	517
	31	13.5	22 (88)	0	100 (405)	493
	31	16.0	13 (48)	0	100 (382)	430
TBAA	31	1.0	0	0	100 (103)	103
	46	1.0	0	0	100 (125)	125
	61	1.0	0	0	100 (78)	78
	76	1.0	0	0	100 (32)	32
	31	1.0	0	0	100 (110)	110
	31	3.5	0	0	100 (114)	114
	31	6.0	0	0	100 (114)	114
	31	8.5	0	0	100 (101)	101
	31	11.0	0	0	100 (71)	71

ages (Table 1). Except for MCAA these ions are much less abundant, usually $< 5\%$ relative abundance, in spectra measured with the TOF system (Figure 1 and Table 2). The differences in the abundances of these ions in the two instrument systems, under otherwise identical solution conditions, are probably related to differences in the designs of the two interfaces, including the diameters of the openings at the spray tips, and the

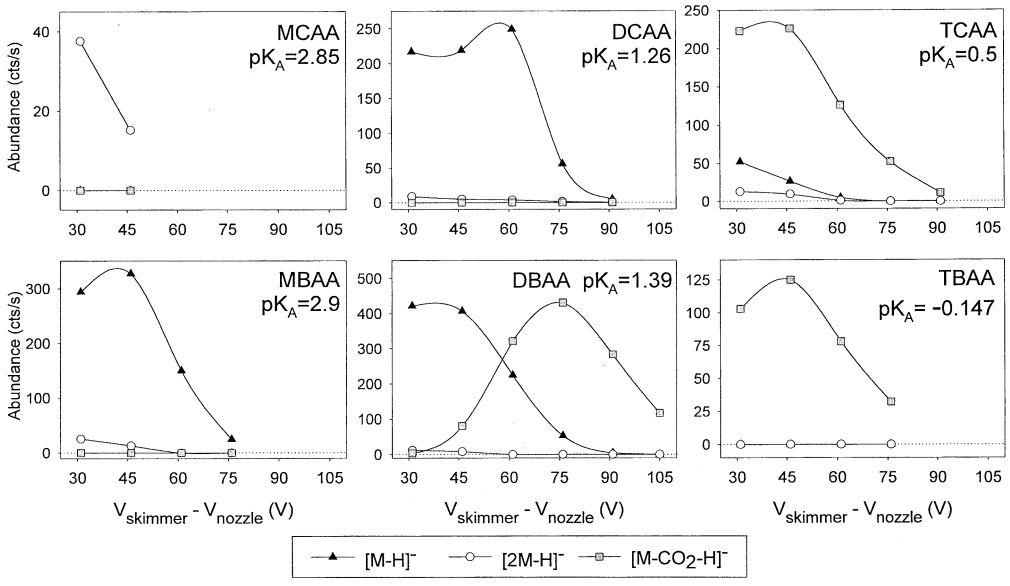

Figure 1. The absolute abundances of the negative ions in the ES mass spectra of six halocetic acids in 50% (v/v) methanol–water at pH 10 measured with the TOF instrument system as a function of the difference between the nozzle and first skimmer potential ($V_S - V_N$).

resulting size distributions of the aerosol particles. Another factor may be the nonoptimal positioning of the spray tip in the TOF system to prevent saturation of the instrument electronics. The design used with the TOF instrument system appears to be more efficient in decomposing proton bound dimers by CID.

The acid TCAA, which is stronger than DCAA, is expected to give abundant $(M–H)^-$ ions but the trend is

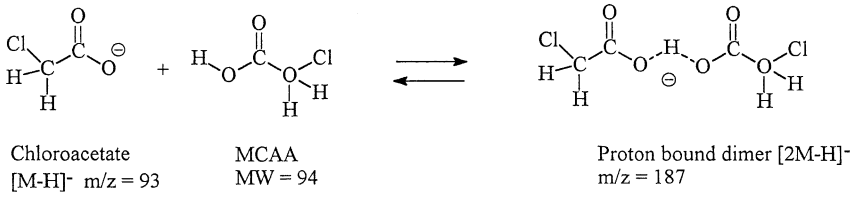

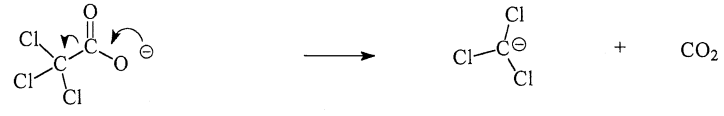

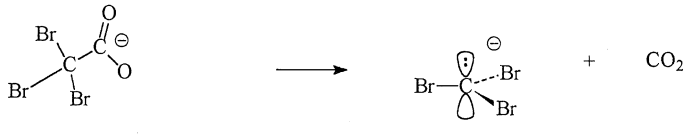

Scheme 2

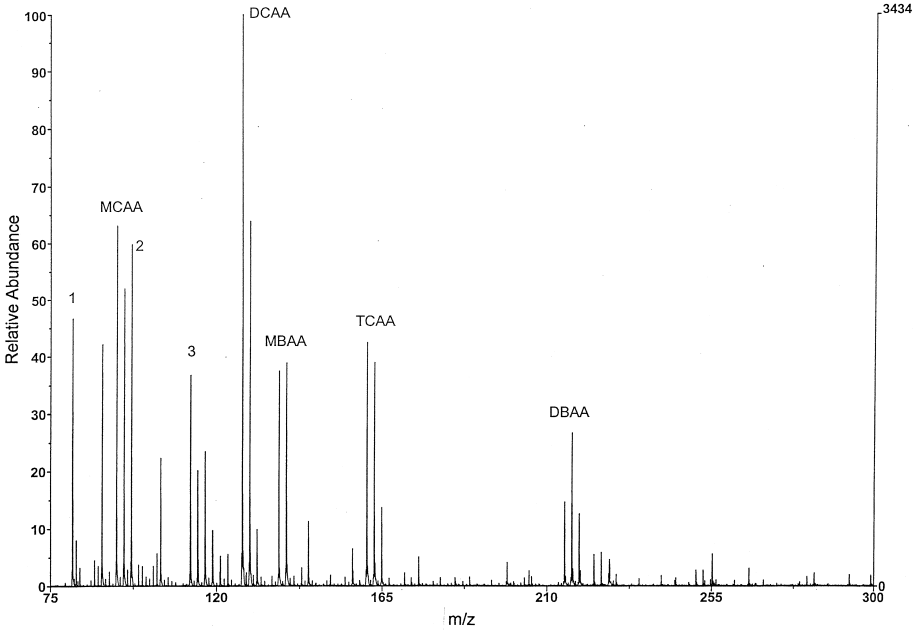

Figure 2. The spectrum of a mixture of the six acids in Table 2 at 100 ppb in 50% acetonitrile–water at pH 10. The ions from the five measurable acids are listed in Table 4 and some of the background ions are HSO_3^- (1) at *m/z* 81, HSO_4^- (2) at *m/z* 97, and $F_3C–COO^-$ (3) at *m/z* 113.

interrupted by the decarboxylation reaction, shown in the second reaction in Scheme 2, to give $(M–CO_2–H)^-$ ions (Tables 1 and 2 and Figure 1). Unlike the other acids, the decarboxylation of TCAA is particularly sensitive to the flow rates of the oxygen sheath gas and nitrogen drying gas. These flow rates were set to the values given in the Experimental section and used for all experiments with all the acids.

The compound MBAA, which has about the same pK_a as MCAA, gives similar absolute abundances of proton bound dimers with the TOF system (Table 2 and Figure 1). Unlike MCAA, however, it gives very abundant $(M–H)^-$ ions at the lower $V_S - V_N$ and $V_Q - V_S$ values (Table 2 and Figure 1). The stronger acid DBAA gives slightly more abundant $(M–H)^-$ ions than the weaker MBAA as expected at the lower $V_S - V_N$ and $V_Q - V_S$ values, but at higher values the decarboxylation reaction reduces the abundance of the $(M–H)^-$ ions. The decrease in abundance of the DBAA $(M–H)^-$ ions parallels the increase in abundance of the DBAA $(M–CO_2–H)^-$ ions (Figure 1) while the total ionization is about the same as indicated by the values of N_{mono} in Table 2. Decarboxylation of DBAA and not DCAA is likely promoted by the larger bromine atom substituents compared to the smaller chlorine atoms. With the strongest acid, TBAA, decarboxylation of the $(M–H)^-$ ion is the dominant process even at low $V_S - V_N$ and $V_Q - V_S$ values (Table 2 and Figure 1). This transformation is the last reaction in Scheme 2 and is likely strongly favored by the relief of steric strain in the transition state from the tetrahedral sp^3 $(M–H)^-$ ion to the planar sp^2 tribromocarbanion.

The Effect of a Lower Concentration of Analytes and an Acetonitrile–Water Matrix

The TOF system is capable of detecting the haloacetic acid negative ions at concentrations lower than the quadrupole system, and the ES from acetonitrile–water mixtures is generally more stable than the ES from methanol–water mixtures. Acetonitrile has a lower viscosity and a lower surface tension than methanol, which may account for this improved performance. A solution of the six acids was prepared with each acid at 100 ng/mL (100 ppb) in 50% acetonitrile–water at pH 10. This concentration, which is a factor or 500 less than the concentration used in the methanol–water solutions, was selected because it produced reasonably strong ion abundance counts, but there was no detector saturation when the spray needle position and other interface adjustments were optimized for maximum ion abundances. Regardless of solvent, the optimum values of $V_S - V_N$ and $V_Q - V_S$ for the TOF system are 31 and 1 V, respectively (Figure 1 and Table 2). Figure 2 shows the spectrum of the mixture of the six acids at 100 ppb in 50% acetonitrile–water at pH 10.

Ions from TBAA were not detected at 100 ppb in acetonitrile–water, but ions from the five regulated haloacetic acids were readily observed (Figure 2). The failure to detect TBAA is of little current importance because it is not regulated and it is relatively unstable in water at ambient temperatures [11]. Significantly, the propensity of some $(M–H)^-$ ions to form proton bound dimers or decarboxylate, which was observed at 50 ppm in methanol–water (Table 2 and Scheme 2) was

repressed, and mainly $(M–H)^-$ ions were observed at 100 ppb in acetonitrile–water. For example, MCAA produced only $(M–H)^-$ ions (Figure 2), but the ratio of the abundances of *m/z* 93 and 95, which should be about 3:1, is distorted by an interference at *m/z* 95, which may be methanesulfonate $H_3C–SO_3^-$ (94.980 83 or 93 ppm from the MCAA anion). This ion could be an impurity in reagent water de-ionized with a sulfonated ion exchange resin or an atmospheric contaminant absorbed by the basic solution. Therefore only *m/z* 93 was used for the measurements of MCAA. A partially resolved interference is also observed at the *m/z* 139 ion of MBAA and these interferences are discussed in a subsequent section. The compound TCAA, which gave base peak $(M–CO_2–H)^-$ ions in methanol–water at 50 ppm (Figure 1 and Tables 1 and 2), produced base peak $(M–H)^-$ ions at 100 ppb in acetonitrile–water (Figure 2). The reasons for the greater stability of the $(M–H)^-$ ions at the much lower concentration in acetonitrile–water are not obvious, but it is reasonable to expect diminished proton bound dimers at the lower concentration. Several other background ions from the de-ionized water or other sources are observed and some of these are identified in the caption of Figure 2. One of these ions is from trifluoroacetic acid which is used as an exact *m/z* calibration compound. The trifluoroacetate ion at *m/z* 113 either is not efficiently removed from the system or is measured with extraordinary sensitivity because it was not present in the mixture analyzed to produce Figure 2.

The detection limits of the five regulated acids in drinking water, without a preconcentration step, are estimated to be in the range of 24–86 ppb with DCAA having the lowest detection limit and DBAA the highest. The acids MCAA, TCAA, and MBAA have intermediate detection limits. These conservative estimates are extrapolations from the observed signal/chemical noise in Figure 2 to a generally accepted signal/chemical noise of the three at the instrument detection limit. The signal/chemical noise of DCAA, measured using the abundance of the *m/z* 127 ion, is about 25 and the corresponding ratio for DBAA, using *m/z* 217, is about 7. The generic background chemical noise, which neglects the more abundant specific background ions identified previously, was taken as a maximum of 4% relative abundance for these calculations. Electronic noise is very low and is not a significant factor as the concentrations of the acids are decreased. Assuming the generic background chemical noise remains about the same, or increases to no more than 4% as the concentrations of the individual acids are decreased, the detection limits for DCAA and DBAA in the 50% acetonitrile–water solution are about 12 and 43 ppb, respectively. These limits are then doubled to account for the dilution factor when 1 mL of water sample is mixed with 1 mL of acetonitrile. The equipment and techniques used in this research are not capable of measuring, without some preconcentration of the sample, several of the regulated haloacetic acids at concentrations found in drinking water. It is reasonable to assume that improved interface and spectrometer designs will soon provide more appropriate detection limits. One probable near term improvement to the TOF system is the ability to use a shorter *m/z* range, which provides greater sensitivity, and simultaneously obtain accurate *m/z* measurements. This issue is discussed in a subsequent section.

Evaluation of Exact Mass Measurements With a Time of Flight Mass Spectrometer

The TOF system is capable of exact *m/z* measurements which could provide strong supporting evidence for an identification when no retention time data from an on-line separation is available and only $(M–H)^-$ ions are observed in an ES mass spectrum. While on-line separations are almost universally used in chemical analyses, there are some significant advantages to bypassing an on-line separation including the reduced time required for an analysis and the potential for rapid real time measurements needed in process control and other applications. The capability of the TOF system for exact *m/z* measurements was evaluated with the mixture of the six haloacetic acids at 100 ppb in 50% (v/v) acetonitrile–water at pH 10. The $(M–H)^-$ ions of the five regulated acids, which are observable at this concentration, were used for all the exact *m/z* measurements and ions containing several combinations of bromine and chlorine isotopes were measured for DCAA, TCAA, and DBAA. The mass spectrometer resolving power was monitored for all exact *m/z* measurements by measuring the full peak width of each ion at half peak height. The resolving power was generally in the 3500–4000 range but occasionally reached about 5000. This resolving power ensures that some potential interferences with the same nominal *m/z* are not measured as haloacetic acids (see later section titled *Potentially Interfering Anions*).

Several techniques were evaluated for the calibration of the *m/z* scale for exact *m/z* measurements. The solution of the six analytes was fortified with 50 ng/mL (50 ppb) of each of four internal standard (IS) calibration compounds whose names and structures are shown in Scheme 3. Also shown in Scheme 3 are the exact *m/z* of the IS ions used to calibrate the *m/z* scale. These compounds were selected from among approximately 20 carboxylic acids and acidic phenols that were evaluated. Evaluation criteria included chemical purities as purchased, propensities to form negative ions in solution, solubilities in the solvent mixture, the *m/z* of their negative ions, the range of *m/z* required, potential interactions with the analytes and other IS ions, and the absolute abundances of the negative ions produced during electrospray with the TOF system. The four compounds selected provide a range of *m/z* that includes most of the *m/z* values of the regulated haloacetic

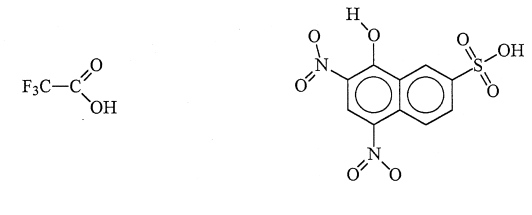

Trifluoroacetic acid
[M-H]- 112.98559

Flavianic acid
[M-2H]-2 155.98497

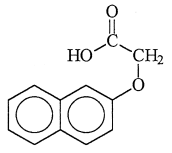

2-Naphthoxyacetic acid
[M-H]- 201.05572

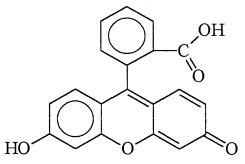

Fluorescein
[M-H]- 331.06120

Scheme 3

acids. The concentrations of the IS were selected to give ions with abundances similar to the acid analytes.

An alternative to the calibration compounds in Scheme 3 are a series of bicarbonate ions (*m/z* 61) associated with *n* water molecules where *n* = 1–30 or more, that is *m/z* 79, 97, 115, 133, etc., which are observed when the sheath and drying gases are temporarily removed after acquisition of the analyte anion spectra (Figure 3). These hydrated bicarbonate ions are produced by the equilibrium of carbon dioxide with hydroxide ion in solution and provide a series of convenient reference ions for calibration of the *m/z* scale. Trace quantities of carbon dioxide are present in the de-ionized water and carbon dioxide may also be absorbed into the basic analyte solutions from the atmosphere during normal handling. This identification was verified by analyzing a solution of ammonium bicarbonate using normal flows of nebulizing and drying gases and the same spectrum as displayed in Figure 3 was observed. The hydrated bicarbonate ions have the

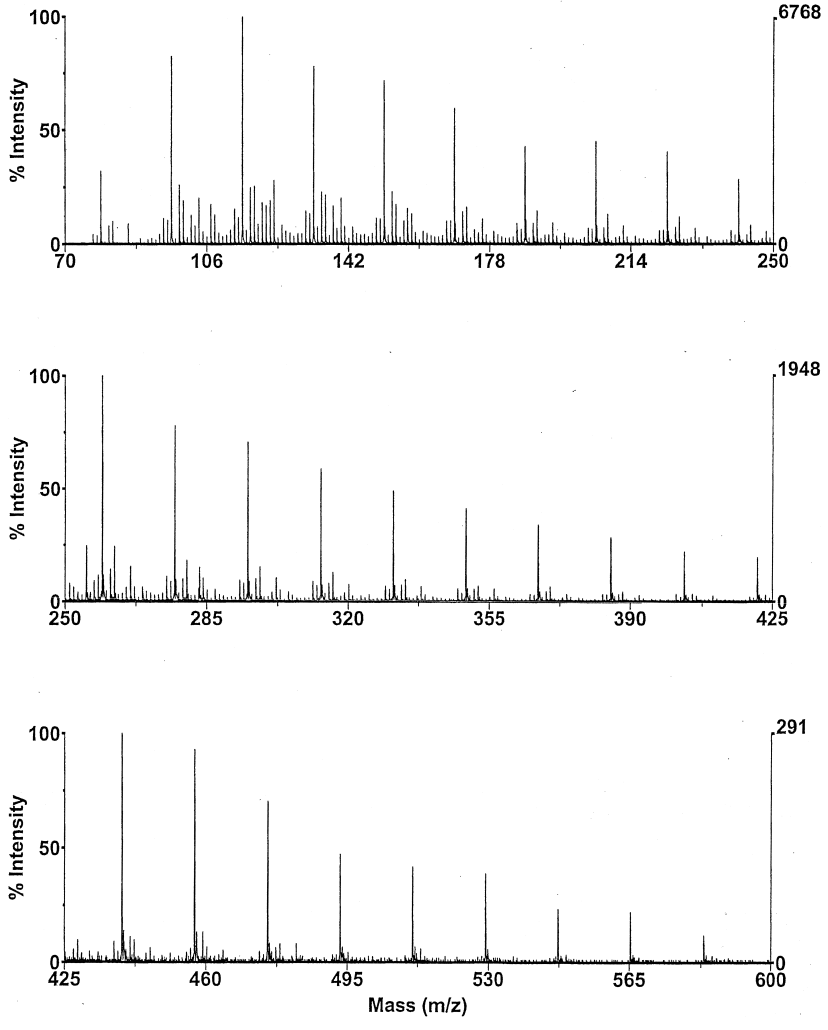

Figure 3. The negative ion ES mass spectrum of hydrated bicarbonate ions in 50% (v/v) acetonitrile–water measured with the TOF instrument system without an oxygen sheath gas or a nitrogen drying gas. The prominent ions in this spectrum are listed in Table 3.

Table 3. Calculated exact masses of the hydrated bicarbonate ions used for *m/z* calibration

$n(H_2O)$	*m/z*
1	79.003 68
2	97.014 25
3	115.024 81
4	133.035 38
5	151.045 94
6	169.056 51
7	187.067 07
8	205.077 64
9	223.088 20
10	241.098 76
11	259.109 33
12	277.119 89
13	295.130 46
14	313.141 02
15	331.151 59
16	349.162 15
17	367.172 72
18	385.183 28
19	403.193 85
20	421.204 41
21	439.214 98
22	457.225 54
23	475.236 11
24	493.246 67
25	511.257 23
26	529.267 80
27	547.278 36
28	565.288 93
29	583.299 49
30	601.310 06

advantage of providing a reference ion every 18 Da but the disadvantage that they are measured about 10 s before or after the analyte measurements under slightly different experimental conditions [12]. Regardless of the calibration standards used, the exact masses of the reference ions and test analytes were calculated by summing the exact masses of the nuclides in the compounds and subtracting the mass of a proton rather than a hydrogen atom. The mass of the electron is significant in some of the lower *m/z* ions and can contribute up to 4 ppm in mass to some ions.

The IS and hydrated bicarbonate ions were employed in two ways to determine the exact masses of the analyte anions. In one approach the exact *m/z* scale is calibrated with a four-point linear regression on the calculated IS exact masses (Scheme 3) or the calculated exact masses of typically 18 of the hydrated bicarbonate ions (Table 3). Alternatively, the exact masses of the analyte anions were determined by a linear interpolation using the exact masses of the two IS ions or two hydrated bicarbonate ions that bracket the *m/z* of the analyte anion. However MCAA could not be measured with the IS two-point linear interpolation because no IS ion is available at $< m/z$ 93.

During the evaluation of the exact *m/z* measuring capabilities of the TOF system, it was discovered that the mass range selected for data acquisition had a significant impact on the accuracy of some *m/z* measurements. When the mass range with the lowest maximum *m/z* available with the instrument was selected, that is 10–4000 *m/z*, very good sensitivity was observed but unacceptable *m/z* measurement errors in the range of 25–100 ppm were obtained for ions at the low end of the spectrum [12]. These errors are not random but follow a trend with *m/z* that suggested they were related to some physical process. When a mass range with a higher maximum *m/z* was selected, for example 10–9000 *m/z*, acceptable *m/z* measurement accuracy and precision were obtained but sensitivity was not as good. The mass range selected controls the idle time between pulses of ions from the ion source into the flight tube and to the detector. The duration of the idle time increases with a longer mass range to allow observation of heavier ions that have longer flight times. A relatively short *m/z* range causes the highest pulsing rate, the best sensitivity, and the greatest *m/z* measurement errors. A longer mass range causes a lower pulsing rate, lower sensitivity, and generally acceptable *m/z* measurements. The *m/z* measurement errors are attributed to a capacitive coupling between the pulsing electrodes and the accelerating stack which impacts most severely ions of low *m/z* [13]. For all subsequent measurements and all data reported in this article the mass range employed was 10–9000 *m/z*.

Table 4 shows the means of ten 10-s measurements of the *m/z* of one or more ions from the five regulated haloacetic acids using each of the four *m/z* scale calibration techniques. Two or three of the isotopic $(M–H)^-$ ions were measured for DCAA, TCAA, and DBAA but only one MCAA and MBAA ion was measured because of the partly resolved or unresolved but detectable interferences at *m/z* 95 and 139, respectively. The ten measurements of each ion were made with the same solution of analytes on five consecutive days with one measurement made near the beginning of each day and another near the end of each day. The range below each mean measured *m/z* is the 99% confidence interval from the Student distribution for $n - 1$ or nine degrees of freedom. Over a large number of samples this interval will contain the unknown population mean 99% of the time. The mean errors in Table 4 are the means of the differences between the calculated anion *m/z*, which is shown in the first column on the far left, and each measured *m/z*. Again the range below each mean error is the 99% confidence interval.

With the exception of the two measurements of MCAA using the hydrated bicarbonate ions as calibration standards, all of the mean errors are less than $\pm$ 9 ppm and the majority are less than $\pm$ 5 ppm. The grand mean measurement error for each calibration technique was also calculated and is shown in Table 4 along with the grand 99% confidence interval. An analysis of variance was conducted to determine whether there are statistically significant differences in the calibration techniques. Again with the exception of the two measurements of MCAA using the hydrated bicarbonate

Table 4. Mean measured exact *m/z* of haloacetic acid anions with 99% confidence limits using four exact *m/z* calibration techniques and mean errors with 99% confidence limits

Analyte calculated	Mean measured *m/z* (n = 10)				Mean error (ppm)			
	Calibration compounds		Hydrated bicarbonate ions		Calibration compounds		Hydrated bicarbonate ions	
	4 point	2 point	18 point	2 point	4 point	2 point	18 point	2 point
MCAA	92.974 18	[a]	92.976 27	92.976 53	− 7.5	[a]	15	18
92.974 88	± 0.000 60		± 0.000 53	± 0.000 36	± 6.4		± 5.6	± 3.9
DCAA	126.935 47	126.936 27	126.936 46	126.935 77	− 3.5	2.9	4.3	− 1.1
126.935 91	± 0.000 37	± 0.000 38	± 0.000 85	± 0.000 87	± 2.9	± 3.0	± 6.7	± 6.9
DCAA	128.932 86	128.933 61	128.933 78	128.933 17	− 0.72	5.1	6.4	1.6
128.932 96	± 0.000 56	± 0.000 51	± 0.000 92	± 0.001 02	± 4.3	± 4.0	± 7.1	± 7.9
MBAA	136.923 88	136.924 38	136.924 51	136.924 53	− 3.5	0.11	1.0	1.2
136.924 36	± 0.000 95	± 0.001 02	± 0.001 01	± 0.000 99	± 6.9	± 7.5	± 7.4	± 7.2
TCAA	160.898 09	160.897 64	160.897 78	160.897 68	7.2	4.4	5.3	4.6
160.896 94	± 0.000 83	± 0.000 75	± 0.001 27	± 0.001 75	± 5.2	± 4.6	± 7.9	± 11
TCAA	162.894 84	162.894 32	162.894 46	162.894 07	5.3	2.1	2.9	0.49
162.893 99	± 0.000 84	± 0.000 82	± 0.001 12	± 0.001 50	± 5.2	± 5.1	± 6.9	± 9.2
DBAA	214.836 07	214.833 65	214.833 44	214.833 47	5.6	− 5.7	− 6.7	− 6.5
214.834 88	± 0.000 81	± 0.000 79	± 0.001 71	± 0.001 54	± 3.8	± 3.7	± 8.0	± 7.2
DBAA	216.834 47	216.832 46	216.831 74	216.831 98	7.6	− 1.7	− 5.0	− 3.9
216.832 83	± 0.000 87	± 0.001 58	± 0.001 80	± 0.001 43	± 4.0	± 7.3	± 8.3	± 6.6
DBAA	218.831 71	218.829 32	218.828 80	218.829 24	4.3	− 6.7	− 9.0	− 7.1
218.830 78	± 0.000 77	± 0.000 78	± 0.001 49	± 0.001 30	± 3.5	± 3.6	± 6.8	± 5.9
Grand mean					1.6 ± 2.3	0.1 ± 2.1	1.6 ± 3.3	0.8 ± 3.4

[a] Bracketing calibration *m/z* not available.

ions as calibration standards, there are no statistical differences in the four calibration techniques.

Potentially Interfering Anions

The resolving power used in the exact *m/z* measurements may separate some potential interferences, but ions with small *m/z* differences from the haloacetic acids could provide erroneous results. Interferences may be detected by larger than expected *m/z* measurement errors, a distorted peak shape, an unusually broad peak, or incorrect ratios of abundances of analyte ions caused by the Br and Cl isotopes. If the error in the measurement of the exact *m/z* of an acid anion in a sample is within the expected error range, that is ± 9 ppm, the peak shape shows no shoulders or splitting, the resolving power is in the normal range, and the ratios of the abundances of the ions caused by Br and Cl isotopes are in reasonable agreement with expected values, there is solid evidence for the presence of the analyte and no interferences are indicated.

If, however, the *m/z* measurement error is > than ± 9 ppm or one of the other indications of an interference is present, then an unresolved anion is probably present. In order to estimate the potential for interfering anions, a graphical mathematical model was developed to determine the maximum difference that must be considered between the *m/z* of an analyte ion and the *m/z* of potential interferences. In this model it is assumed that peak shapes are Gaussian and that measurement errors of ± 15 ppm or greater, which are close to the largest mean error in Table 4, would be an immediate cause for suspicion that an interfering ion was present. With an error of this magnitude or larger, the identification of the analyte is uncertain and the peak area should not be trusted to represent only the analyte ion. This model indicated that errors smaller than 15 ppm could be caused by interfering ions with *m/z* within ± 200 ppm of the calculated analyte *m/z* if the interference was present in amounts ranging from 10 to 100% of the amount of the analyte ion. Furthermore interfering ions with these characteristics may not affect peak shape, resolution, or isotope ion ratios enough to be recognized. Therefore compositions with calculated *m/z* within ± 200 ppm of the calculated analyte *m/z* are potential interferences if they could reasonably be expected to form negative ions in aqueous acetonitrile under ES conditions.

A search for potentially interfering negative ions was conducted by calculating combinations of C, H, O, N, F, Cl, Br, I, S, P, and Si that have an exact *m/z* within ± 200 ppm of the calculated exact *m/z* of the ions in Table 4. The combinations were determined and their *m/z* calculated, evaluated, sorted, and printed using a computer program written for this research in the C language. The number of combinations found by the program was constrained by limiting the number of atoms of each kind to a reasonable number for each *m/z*. Only the major isotopes of C, H, O, N, S, and Si were used in the calculation and only compositions containing at least one oxygen or one sulfur atom to carry the negative charge were considered. Since all the even-

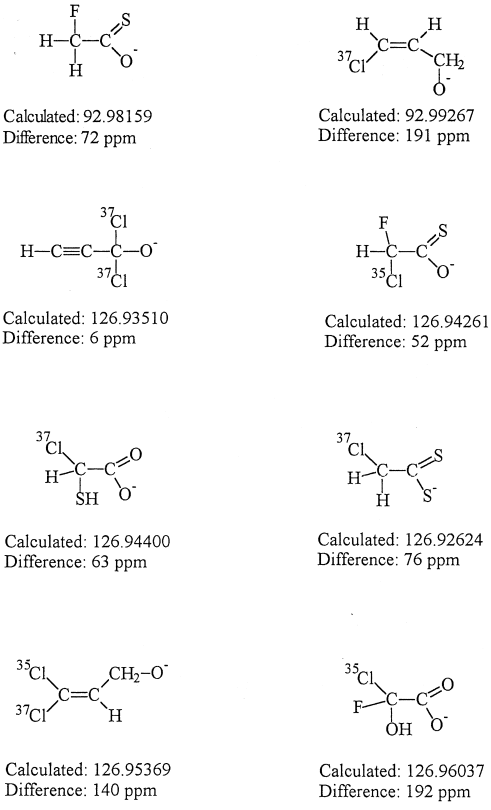

Scheme 4

electron $(M–H)^-$ ions in Table 4 have an odd mass and only even-electron anions with an even number of nitrogens can have an odd mass, only compositions containing an even number of nitrogens were considered. The compositions found by the program were examined individually for viable chemical entities that can be reasonably expected to form negative ions in aqueous acetonitrile under ES conditions.

Scheme 4 contains the structures, calculated *m/z*, and differences in ppm of the singly charged anions that could conceivably interfere with measurements of MCAA and DCAA at *m/z* 93 and 127, respectively. While these compounds are not typical natural products or commercial materials, they are viable structures that could be present in waste discharges or raw sources of drinking water. If present in appropriate amounts, these anions would not be resolved from the MCAA and DCAA $(M–H)^-$ ions but they would, depending on the relative amounts, distort the abundance ratios of the MCAA and DCAA isotope ions, distort peak shapes, and cause variable errors in exact *m/z* measurements. Three of the ions in Scheme 4 are allyl or related alcohols and it is unlikely they would be sufficiently acidic to form appreciable concentrations of negative ions in solution. Seven of the eight substances contain one or more Cl atoms and therefore isotope ions would be present at ± 2 Da, which would distort ratios of abundances of MCAA and DCAA isotope ions. At the higher *m/z* used to measure TCAA, MBAA, and DBAA more potential interferences exist but similar uncommon structures are potential interferences and the same conclusions can be drawn concerning the recognition of these interferences when present. None of the substances in Scheme 4 have been found in drinking water samples but no drinking water samples have been examined using the techniques described in this article.

Conclusion

Electrospray with the bench-top TOF mass spectrometer and exact *m/z* measurements at resolving powers in the 3500–5000 range has the potential of forming the basis for an extremely simple analytical method for determination of the regulated haloacetic acids in drinking water. The potential method could provide useable results within a few minutes compared to existing methods which require considerable sample processing and GC. The estimated detection limits without a sample preconcentration step are within about a factor of 10 of those required for measurement of the regulated haloacetic acids in drinking water samples. It is reasonable to expect sufficient improvements in equipment and techniques to achieve the needed detection limits in the near future. No drinking water samples were analyzed pending the development of slightly more sensitive techniques and quantitative analytical procedures. A thorough study of the precision and accuracy of the potential method is required before it should be considered for measurements of the haloacetic acids in drinking water.

Acknowledgments

This research was supported in part by an appointment of Olivier Debré to a postdoctoral research associateship administered by the National Research Council through a cooperative agreement with the U. S. Environmental Protection Agency. This research was also supported in part by an appointment of Xinbei Song to a postdoctoral research fellowship administered by the Oak Ridge Institute for Science and Education through an interagency agreement between the U. S. Department of Energy and the U. S. Environmental Protection Agency. The authors express their appreciation to Phil Epstein of PE Biosystems for his generous assistance in providing the Mariner system for evaluation and use in this research. The authors also thank Larry Wymer, USEPA statistician, who conducted the analysis of variance and Elizabeth Hedrick, USEPA chemist, who provided comments and advice on the statistical evaluation of the calibration techniques.

References

1. Krasner, S. W.; McGuire, M. J.; Jacangelo, J. G.; Patania, N. L.; Reagan, K. M.; Aieta, E. M. *J. Am. Water Works Assoc.* **1989,** *81*, 41–50.
2. *Federal Register* **1994,** *59*, 38668–38829.
3. *Federal Register* **1998,** *63*, 69390–69476; Title 40 Code of Federal Regulations Parts 9, 141, and 142.
4. Method 552 in *Methods for the Determination of Organic Com-*

pounds in Drinking Water Supplement I; EPA-600/4-90/020; Washington, DC, 1990, 201–232.
5. Method 552.1 in *Methods for the Determination of Organic Compounds in Drinking Water Supplement II*; EPA/600/R-92/129; Washington, DC, 1992, 143–172.
6. Method 552.2 in *Methods for the Determination of Organic Compounds in Drinking Water Supplement III*; EPA/600/R-95/131; Washington, DC, 1995.
7. Fenn, J. B.; Mann, M.; Meng, C. K.; Wong, S. F.; Whitehouse, C. M. *Science* **1989,** *246*, 64–71.
8. Banks Jr., J. F.; Dresch, T. *Anal. Chem.* **1996,** *68*, 1480–1485.
9. Bruins, A. P.; Covey, T. R.; Henion, J. D. *Anal. Chem.* **1987,** *59*, 2642–2646.
10. *Lange's Handbook of Chemistry*, 14th ed.; McGraw-Hill, New York, 1992.
11. Cowman, G. A.; Singer, P. C. *Environ. Sci. Technol.* **1996,** *30*, 16–24.
12. Debré, O.; Budde, W. L. *Proceedings of the 47th ASMS Conference on Mass Spectrometry and Allied Topics*; Dallas, TX.
13. Peltier, J. M.; Takach, E.; Zhou, J.; Chen, X.; Gabeler, S. *Proceedings of the 47th ASMS Conference on Mass Spectrometry and Allied Topics*; Dallas, TX.